*Pure & Appl. Chem.*, Vol. 66, No. 6, pp. 1319–1326, 1994.
Printed in Great Britain.


# Nucleation, growth, and morphology of dust in plasmas

**Alan Garscadden, Wright Laboratory**

**Wright-Patterson Air Force Base, Ohio, U.S.A.**

**Abstract:** An account is given of the dust particles appearing in weakly ionized plasmas. The dust is found in many discharges, especially in electronegative gas plasmas under conditions of rf excitation similar to those used in plasma processing of integrated circuits. Measurements have been made of the plasma-trapped dust, interrogated by Mie scattering of laser light. It appears that the rapid early growth is controlled by ion accretion across the surface of the relatively large Debye sheath. The microscopic properties of the dust reveal that the particles are often almost monodispersive in size. Under some conditions, the dust morphology has fractal characteristics and considerations of growth conditions point to the critical role of negative ions and ion-assisted deposition

## 1.Introduction.

Dust occurs ubiquitously in many plasmas including astrophysical plasmas, combustion, gas lasers and materials-processing arc discharges. The presence and electrical charging of solid particles in weakly ionized plasmas are important in many technical areas. These areas include aeronomy, thunderstorms, the conductiyity of rocket or engine exhausts, the electrostatic precipitation of particles, and electrostatic effects of condensation in supersonic flows. Grains in space are of special interest because of their importance in forming molecular hydrogen and providing a pathway to more complex molecules. Recent studies (1-5), applying laser probing (Mie scattering) to low pressure rf excited plasma research reactors and to etching and deposition reactors that are used in integrated circuit manufacturing, have shown that particles also often occur in these plasmas, and can adversely affect the manufacturing process and the integrated circuit or material properties.

## 2. Dust in RF Discharges.

The typical parallel plate reactor has electrodes 10-20 cm. diameter separated by 2-10 cm., depending on the gas mixture and wafer process. The etching reactors are usually run at pressures below 0.3 Torr and thin film deposition reactors at a few Torr. The yields of plasma enhanced processing reactors are often degraded by particle formation.The sizes of the cluster or particles that are observed in the reactors range from tens of Angstroms to several microns and, under some circumstances, as large as $10^{-1}$ cm. A typical dust particle of one micron size contains $10^8$-$10^9$ atoms. The particles can be introduced by several mechanisms. These include flaking from the substrate or walls, clustering and polymerization of the gases or substrate materials, sputtered material, ablation, and aerosols from the gas supply. Particles of micron size will be lifted off a surface in relatively small electric fields.

## 3. Experimental Observations.

**(a) nucleation.** We found that dust is readily formed and trapped under conditions of rf excitation and low pressure especially when the discharge approaches the situation of two opposing negative glows. The origin of dust particles in laboratory plasmas therefore has been studied in low pressure discharges under conditions of low rf excitation up to 100 kHz. Glass discharge tubes were used with plane parallel disk graphite electrodes and a variety of electrode sizes and electrode spacings.The electrodes were usually mounted vertically so that on switch-off of the discharge the dust particles fell to the bottom of the chamber and not onto the electrodes. Equal area and up to 4:1 area ratio electrodes have been used. To trap the dust, good radial symmetry of the discharge and electrode alignment were imperative. The discharges were operated without gas flow with selected gas mixtures at a known initial pressure. The discharge volume was interrogated for particles using either a cw argon ion laser operating at 4880 A, or a krypton ion laser at 6401 A. (Fig. 1) Particles rapidly formed throughout the volume in gases (eg CO) where electron impact-induced dissociation produces carbon atoms, and also in inert gas plasmas with carbon electrodes; the material then must originate from the electrodes, by ion- or metastable-induced sputtering (6). These processes increase the vapor pressure of carbon atoms many times over the equilibrium value for the gas temperature. Qualitatively, under such conditions homogeneous nucleation occurs with the critical size for a stable 'cluster' extending to the dimer. The nucleation to a crystallite at high pressures is enhanced by the very large pressure ratio, equivalent to supercooling, and by the presence of ions (7). Recent studies (8) of nucleation in carbon vapor, in connection with fullerene formation, indicate that the intermediate complex $C_3$* is long-lived which improves the formation probability of larger clusters.

However it is doubtful that classical nucleation is applies in a low pressure bounded plasma. Also, our measured early growth rates suggest an ion mechanism that takes advantage of the large Debye sheath collection. The dust density, estimated from the intensity and statistics of the Mie scattering of the laser, is $10^5$ to $10^7$ $cm^{-3}$. Other investigators have reported densities as high as $10^8$ (9). In the CO-Argon mixture, the dust eventually accounts for most of the carbon from the gas. It is quite remarkable that the nucleation and growth to micron size in this discharge occurs on the time scale of seconds, even at mA discharge currents. In pure helium or argon discharges time was of the order of tens of minutes before the grains were observable by laser scattering.

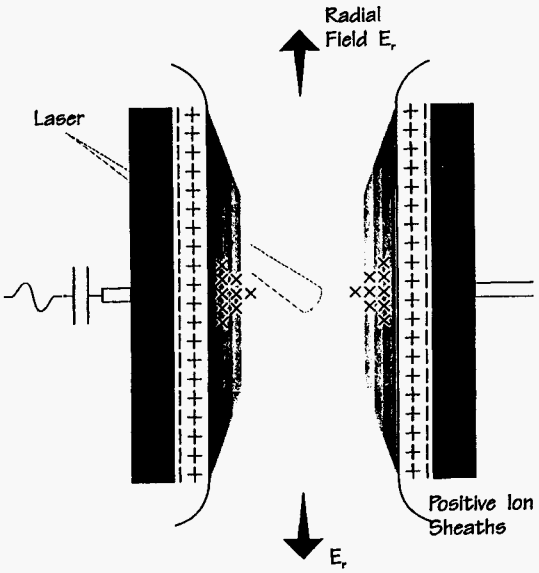


Fig. 1 Laser Interrogation of discharge for dust.

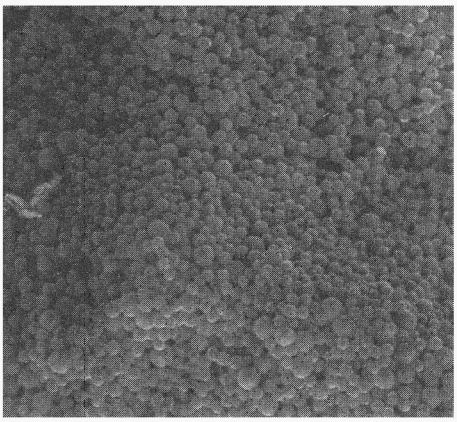

Fig. 2 A 5 keV SEM (8000x) of the dust grains from a 1:5 CO-Ar ).3 torr plasma at 50 kHz.

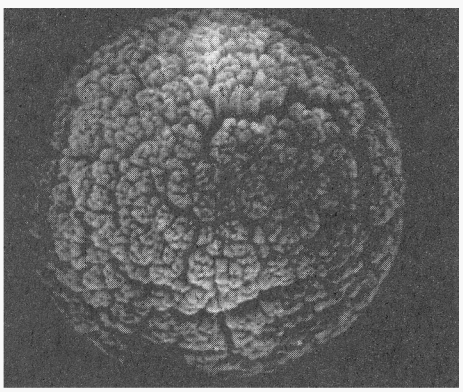

Fig. 3 A 2 keV SEM (110,000x) of a dust grain. Other conditions as in Fig. 2 Note higher resolution of the surface morphology at low beam energy.

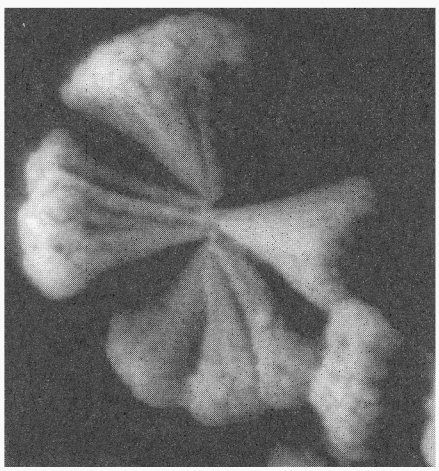

Fig. 4 SEM of a broken grain suggesting fractal growth.

**(b) trapping:** The dust can be easily trapped for hours in the rf excited plasma.This is to be contrasted with the timescales for positive ion diffusion and neutral diffusion, which are on the order of milliseconds. The exclusion of the dust from the sheaths confirms that the dust is negatively charged. The propensity of clustering to occur in electronegative discharges, even at pressures below one Torr, and the long residence time of negative ions in rf plasmas, suggests that negative ion formation is often linked to both the early particle formation and growth into larger particles. Negative ions accumulate in many discharges, even in the silane discharge, which is not particularly electronegative. This is due to the rf discharge configuration and to the negative self-bias on the electrodes that results from the asymmetric discharge response to the rf excitation. Negative ions cannot diffuse to the electrodes or boundaries because of the repelling sheaths and ambipolar fields. They will be lost by recombination and detachment, and as a the negative ion density can build up to values exceeding the electron density. In steady state at low ion densities where recombination is unimportant, the negative ion density $n_- = K_a N_a / K_d$ where $K_a$ and $K_d$ are the attachment and detachment coefficients respectively, and $N_a$ is the density of the attacher. Boltzmann transport calculations for silane-argon mixtures give $K_a/K_d = 10^{-3}$ so that at typical fractional ionizations the negative ion density is up to $10^3$ times the electron density. Howling et. al. (10) using mass spectrometry on silane discharges, found stable negative ions, with up to sixteen silicon atoms. Negative ions and dust particles have significant effects on the plasma properties and plasma chemistry. The electron energy distribution is changed and the plasma impedance is increased (6, 11, 12). The particles provide a dispersed surface that may catalyze recombination of atoms and radicals and, if hot enough in a high energy discharge, cause dissociation of species.

**(c) morphology:** The measurements revealed different types of particles or dust, depending on the gases and the plasma conditions. In gases such as carbon monoxide-argon mixtures, the particles were detected essentially instantaneously (less than a second) on discharge ignition and they were dispersed reasonably uniformly throughout the discharge volume and boundary regions. Ex-situ examination showed that these particles were of remarkably uniform size :- for the example of a discharge in 0.3 torr 20% CO:80% Ar mixture, about 0.7 microns diameter. Figure 2 shows a low energy scanning electron microscope (SEM) image at 8000 magnification of the dust particles extracted from this plasma and sputter coated with ~ 30 A of gold. Increasing the SEM magnification to 35,000 shows that the particles have an open structure and display cauliflower-like patterns representative of diffusion-limited aggregation. Some of the observed asymmetries and break-up of the particles may be caused by the damage due to charging by the electron beam of the SEM. Diffusion-limited growth is well illustrated by SEMs at 110,000x (figure 3). Figure 4 shows a broken particle at the same magnification. A classical fractal growth pattern is also observed in transmission electron microscope (TEM) images. The SEM and TEM photographs and x-ray scattering data show that the material of the dust from the CO-Ar discharges is usually amorphous. If this CO-Ar discharge is run for a long time (hours), or after many on-off cycles, the particles become larger and then tend to be concentrated just outside the electrode sheaths. Segregation effects are also found in electronegative gas discharges or when the particles arise from sputtering of carbon electrodes. In most gases the dust forms at the sheath edge, and then disperses slowly into the plasma. Selwyn et al.(1) have demonstrated that certain chlorine- and fluorine- containing gases (especially in the presence of both gases) for etching plasmas produced dust during etching of a silicon substrate. Simultaneous laser light scattering from the dust and two-photon laser induced fluorescence from ground state chlorine atoms, and photodetachment of negative ions and subsequent fluorescence, showed a strong correlation between the spatial positions of the dust and of the negative ions. If a reactor has gone through many cycles without cleaning, or is subjected to vibration, very large (~0.1 mm) particles can be observed, trapped, in reactive ion etchers. Discharges in silane and silane-rare gas mixtures are especially prone to particle formation at higher pressures and higher powers (13). The dust density increases rapidly with higher pressure and higher power-loading of the discharge. A summary of some of the different conditions where dusty plasmas have been observed in the laboratory is given in Table 1.

**Table1: Correlations and Characteristics of Dust in Laboratory Plasmas**

| GASES | BOUNDARY CONDITIONS | PARTICLES | REFERENCE |
|---|---|---|---|
| $SiH_4$ | No Wafer | Near Sheath Edge | Spears |
| 10% $CCl_2F_2$/Ar | Wafer, Si etch | Yes | Selwyn |
| | No Wafer | No | " |
| 5%$SF_6$9%$Cl_2$/Ar | Wafer, Si etch | Yes | " |
| | $SiO_2$ | Few | " |
| $Cl_2$/Ar | Wafer/No Wafer | No | " |
| 20%CO/Ar | No Wafer | Many | WPAFB |
| Ar or He | Carbon Electrodes | Yes | " |
| He | Al, Mo | Few | " |
| 1%$CH_4$/Ar | - | Many | Graves |
| 5%$CCl_2F_2$/Ne | - | No | Selwyn |
| Ar | $SiO_2$ sputtering | Yes | " |

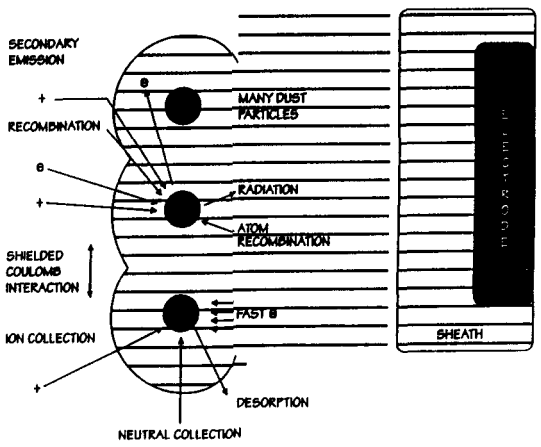


Fig 5. Particles near plasma sheath

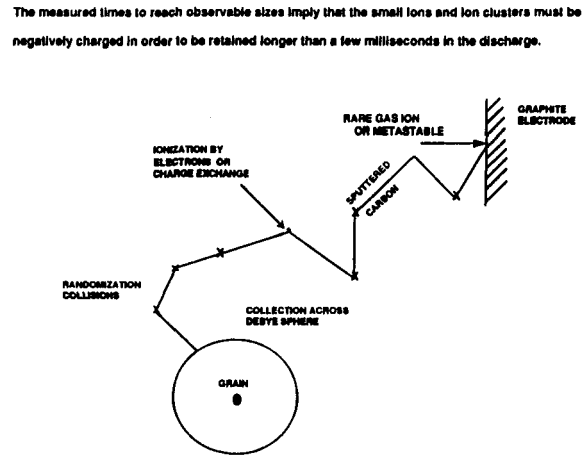


Fig 6 Explanation of high growth rates and long trapping times of Carbon grains at low pressure.

**(d) Particle densities:** The typical laser scattering intensity from the particles in these low pressure discharges is very large, much larger than that from dusty room air and comparable to that from the chamber windows. Provided the discharge geometry is reasonably symmetric, the dust can be trapped for days in the plasma. As the discharge run time increases the particle density usually increases. At high particle densities ( $>10^6$ cm$^{-3}$) new phenomena occur. The particles act collectively, literally like a fluid. On one occasion an extended thin planar structure was observed near a floating Langmuir probe. We have observed the dust at high densities, to form one or more colloid-type forms, while suspended in the plasma. Selwyn (3) has observed similar effects, including regular hemispheres above test wafers. The equilibrium position of the dust is strongly influenced by the electrode surface material and geometry (14).

There are many interactions that result from the presence of a macroscopic particle in a plasma. Some of the more important ones for particles located outside the sheath in a reactive gas discharge are illustrated in figure 5. There are ion, electron and neutral fluxes to the surface of the particle. At high bias potentials the ion bombardment may cause secondary electron emission. The ion and radical recombinations cause particle heating. Under high dust density conditions the particles interact with each other and a separate double layer sheath forms around the dust ensemble.The interactions lead to various constraints on the particles which must be satisfied simultaneously. The constraints include a) the electrical charge, b) the position in the discharge, c) the temperature of the particle, d) the size and growth rate, e) the perturbation of the plasma ionization and chemistry, and f) interactions between the dust particles. Various forces that act on the dust are summarized in Table 2.

**Table 2. Summary of forces on a dust grain in a 1 torr Argon afterglow**

| | | | |
|---|---|---|---|
| $F_{nc}$ | neutral drag | $5.0 \times 10^{-9} r^2 v_f$ (Dynes)<br>$0.00213\ \rho_g r^2 v_f$ | r=radius in microns<br>$v_f$=flow velocity cm/s<br>$\rho_g$=gas density (g/cc) |
| $F_g$ | gravitational | $3.82 \times 10^{-9} r^3 \rho$ | $\rho$=grain density (g/cc) |
| $F_{th}$ | thermophoretic | $1.2 \times 10^{-7} r^2 \nabla T$ | $\nabla T$ in K/cm |
| $F_{es}$ | electrostatic | $1.6 \times 10^{-12} qE$ | q in electronic charges<br>E in V/cm |
| $F_{id}$ | ion drag | $0.137\ JQ$ | Q cross-section in cm$^2$<br>J current density mA/cm$^2$ |
| $F_{pg}$ | pressure gradient | $5.5 \times 10^{-10} r^3 \nabla P$ | $\nabla$ P in torr/cm |
| $F_s$ | stokes force | $4.8 \times 10^{-7} r v_f$ | $v_f$=flow velocity cm/s |

**(e) Particle charging:** We observed that dust is excluded from the rf discharge electrode sheath regions. As these are (time-averaged) negatively biased electrodes; this result indicates that the dust is negatively charged. The dust will be at floating potential in order to equalize the charged particle fluxes. When the radius of the particle is much less than the Debye length, the potential of the particle is 2Z/a. If the particle is large enough that the charge is delocalized, this potential must equal the floating potential. Bulk properties of the material are expected to occur as long as the number of atoms in the cluster exceeds about 200. If the particle is close to a sheath in a low frequency excited discharge, it may intercept fast electrons and float highly negative. In a discharge plasma the floating potential constraint, typically of a few volts, (-2.51 kT for protons and -3.61 kT for ionized oxygen atoms) requires $10^2$-$10^4$ surface electron charges. The dust particles are then very efficient Coulomb scattering centers (9) and can significantly change the transport properties of the plasma and, at high concentrations, deplete the local electron density. Goertz (15), and others (16) have calculated the effects of dust density on the plasma potential and the potential of the dust. As long as the fractional amount of dust compared to the ion density is less than $10^{-6}$, there is little effect. However when the amount of dust exceeds this value, the plasma potential is depressed and the negative floating potential of the dust becomes more positive. A detailed discussion of the electrostatic charge on a dust size distribution in a plasma has been given by Houpis and Whipple (17). The surface charge constraint may be linked to the particle size distribution in that very small particles are not usually observed in electropositive plasmas. If the particle is very small the surface electrostatic forces will exceed the tensile strength of the material and it will fragment. There are limits on the magnitude of charge that a particle can acquire (18,19), , however very high potentials can be reached if the particle is a compact solid. If the particle is a spherical solid, the maximum number of charges is $Z(max) = E_s a^2/4e$ where $E_s$ is the surface field intensity at which emission of ions or electrons occurs. For ions this is approximately $2x10^8$ volts $cm^{-1}$ ; for electrons it is $10^7$ volts $cm^{-1}$. For 1 micron particles these values correspond to $3.5x10^6$ and $1.7x10^5$ electronic charges per particle, respectively. The melting temperatures of microclusters decrease with decreasing size and are much lower than those of the bulk solid. ( the example of gold microclusters is cited where the melting temperature decreases from the bulk value of 1336 $^0$K above 250 A to less than 400 $^0$K below 25 A diameter (20). Material properties such as the effective surface tension of small charged clusters are expected therefore to be weakened, and relatively small numbers of charges and resulting fields will be able to disrupt such particles.

There is a fundamental difficulty in an isolated charged particle maintaining floating potential at very small diameters. However the fact that many particles are formed, perhaps by homogeneous nucleation at the higher pressures means that there will be depletion of the electron density due to the number of electrons needed for the surface charges means that the floating potential will be reduced. To an extent, an energetic plasma with limited dust density is mass-selective: if the particle is too small in an energetic plasma, it will suffer Coulomb explosion; if it grows too large, the electrical fields will not be able to trap it, and gravity eventually wins. Whipple (19), predicted limits on the minimum particle size as a function of the floating potential and of the material. It may be that the maximum size is limited by the amount of material available under the sealed-off gas fill conditions, and of course, eventually by the gravitational field exceeding the radial electric fields of our configuration. These considerations suggest further influences of negative ions on cluster formation and on the stability of charged dust particles:- at high negative ion densities the floating potential is reduced, permitting smaller particles to grow within the active plasma region. Therefore it appears that the initial growth of particles will be favored by the presence of negative ions. Additional reasons for negative ion involvement come from the morphology and growth rates of the particles (6). Figure 6 illustrates the model that is implied by the low pressure sputtering carbon source. In some cases, there may be early growth outside the plasma, and of the particles that drift into the plasma, only those above a minimum size will survive.

**(f) Particle spatial distributions and forces:** The equations for continuity, momentum and energy must be considered for all of the charged species, including the dust and any negative ions. The forces on the particles are those due to the electrical field, a polarization force if the particle is asymmetrically charged, and an ion drag force due to collisions with ions. Also, there are thermophoretic forces if temperature gradients exist in the gas, and the gravitational force. The last is small for typical particle dimensions and materials, and typically is compensated by electrical fields of 0.1-1 volt/cm, i.e. within the ambipolar range. The most important force is the ion drag. Graves (21) has used a screened Coulomb force to describe the collisions with particles. Even when the Debye length is determined (for small particles) by the ion temperature, the resulting cross section values are very large due to the large surface charge (about 1000e) The ion drag force is a sensitive function of the ion velocity and, for the conditions assumed, it is compensated by the electric field close to the sheath boundary, leading to an eventual dust equilibrium position just outside the electrode sheath. The ion density gradient and ambipolar field to the boundary provide ion flow that causes an ion-wind effect on the dust. The opposing electrostatic field on the (negatively) charged dust balances the drag near the plasma sheath boundary. The ion drag force decreases near the boundary due to the increase in ion velocity, while the electric field has increased.

We noted that the presence of dust is often associated with electronegative plasmas and with very low electron energies. If the ion-ion recombination loss or the electron detachment of negative ions is larger than the diffusion loss, then the particle positions for these discharges will be changed by the modified electron and ion gradients. The particles may also be trapped by polarization forces due to the asymmetric charging near the boundary. Static forces result from the rf modulation because the charge density may also oscillate sympathetically at the rf frequency.

**(g) Particle heating:** The particle temperature is determined by the balance between energy gains and the radiation losses which are the dominant energy loss at low pressures (22).The energy equation for the particle contains terms for electron-ion recombination on the grain and the ion bombardment energy, radiation cooling, gas cooling and the net of atom/radical recombination, pyrolysis and desorption. The radiation loss is given by the Stefan-Boltzmann law with a correction for the efficiency of radiation by a particle smaller than the wavelength of the radiation. This raises an interesting point as to exactly how efficient are very small particles in losing energy by radiation At the low pressures of most plasma reactors, Knudsen-type cooling is operative. An additional term in many gases results from atom-atom and/or radical recombination on the surface of the particle. There may also be cooling due to desorption and pyrolysis. While the net result for radical recombination will be only of the order of eV per reaction, the density of radicals is likely to be at least an order of magnitude larger than the ion density. The sum of the ion heating is here taken to be of the order of the ionization energy per recombination, so that an estimate is that the ion and radical heating terms are about equal. Then one obtains heating rates as approximately $10^{-12}$ $n_e$ cal $cm^{-2}$ $s^{-1}$. At electron densities of $10^{11}$, $10^{12}$ and $10^{13}$ the equilibrium particle temperatures (at low pressure, neglecting gas cooling) for an emissivity of 0.6 are 600, 1050 and 1850 K respectively. Heating times are in the range of millisecs for $10^{12}$ ion density, and correspondingly longer for the more usual lower densities. The most important effect of the particle heating is that it may accelerate the dissociation of reactive gases by promoting pyrolysis of the gas on the surface of the particle. Something non-linear of this nature appears to be required to explain the sensitivity of dust production in silane to power loading and pressure. If melting occurs then the maximum surface charge is controlled by the surface tension, otherwise the drop becomes unstable. Under usual energy densities, thermionic emission from the particles in a low pressure rf reactor is not anticipated, but it may occur in higher power sputtering reactors.

## 4. Ionization kinetics.

Conditions for trapping the negative ions and/or dust are especially favorable in an RF discharge because the electrodes are negatively self- biased over most of the rf cycle, and thus repel heavier negatively charged particles completely, as the more mobile electrons satisfy the condition of no net charge collection averaged over the discharge excitation cycle. The radial ambipolar fields also trap these particles. The ion concentration gradients in an electronegative gas discharge are usually quite small over most of the characteristic diffusion length. The ambipolar fields of the electronegative plasma in a particle contamination situation will tend to concentrate some particles on axis, given sufficient time for the particles to drift to the center of the discharge (assumed symmetric excitation). We observe this effect more clearly with the discharge axis horizontal. If the line density of dust is such that there is sheath interaction between the particles, or if the recombination loss is large on these particles, then the dust ensemble forms a new boundary condition for the plasma. Since the dimension of the perturbation is actually determined by the Debye length and the diffusion lengths within the plasma, and not by the dimensions of the particles, relatively few particles are required to exact a new boundary condition. The dust volume is often crisply defined.The dust at the boundary of the trapped volume interacts with the surrounding plasma however the interior dust is shielded from the plasma and the electron energy distribution can be significantly different. One expects that the mean energy will be lower, resulting in a lower floating potential for the interior dust. Such effects may explain the apparent structures that are formed. If the particle is already negatively charged, then on switch-off or modulation of the plasma, the floating potential will decrease as the electron temperature decreases. When the electron density decays to a value such that the volume of interest actually becomes a sheath and free diffusion occurs, the electron density can fall below the ion density. The dust may then charge slightly positive in the afterglow.

## 5. Chemical Kinetics:

It is noted that the geometric surface area of 1 milligram of silicon of spherical particles of 0.1 micron in diameter equals approximately 230 $cm^2$, often exceeding the electrode areas.The fractal structure means that the actual area may be much higher. Once formed, such particles have low diffusion coefficients relative to the electrons and ions (e.g. a micron diameter sphere will have a diffusion coefficient of approximately $3x10^{-4}$ $cm^2$/sec at 1 torr). The particles become distributed sinks for recombination of charged species and radicals. Recombination of atoms and radicals will often be accelerated by three body recombination on the surface of the dispersed condensed phase particles. When two atoms bind, some of the recombination energy will be deposited to the particle. Analyses of association on grains has been a topic of interest in

astrophysics for many years (23). Recombinations and associations promoted by the dust acting as a third body are considered to be the source of the interstellar molecules, both molecular hydrogen and the more complex molecules.

## 6. Collective effects

From the laser scattering intensities from the discharge dust compared to room air the particle density is believed to reach $10^5$ - $10^6$ $cm^{-3}$. When the rf driving voltage is high enough the dust density builds up and sharply delineated volume become observable in the laser scattering. These volumes respond to perturbations with a response of a few hertz. If a dust particle is in the vicinity of a plasma boundary (rf electrode) that, at lower frequency excitation, injects fast electrons into the plasma, then the floating potential of the particle will be approximately the magnitude of the peak applied voltage. Under these circumstances the number of elementary charges on the particle should be of the order of $10^5$. However, locally the electron density near the particles must be severely depressed, because the product NZ approaches the electron density. The impedance of the discharge may increase, however, often the discharge takes the lowest impedance path available and simply goes around the dust if the configuration permits it.

The normalized coupling constant describing the interaction between the charged macroscopic particles (ratio of Coulomb energy to thermal energy, $\Gamma = Z^2e^2/dT$, where d=interparticle distance) can be large in this situation because the coupling scales with $Z^2$. This can be rewritten as $\Gamma = 2.7\ 10^{-5}Z^2(N/10^{12})^{1/3}(10^6/T)$, where T is the particle temperature ($^0K$) and N is the dust number density ($cm^{-3}$). If the coupling constant is between 4 and 170, it is predicted, (24) that phase condensation of the dust to a liquid will occur, and if it considerably exceeds 170 then a Coulomb solid is expected (25). The required density is $N= 5.10^7\Gamma^3T^3Z^{-6}$. A typical low pressure discharge ion-electron plasma with T= 10,000 $^0K$ and Z =1 would require $N = 5.\ 10^{19}$ to make $\Gamma = 1$. Although our dust densities are relatively low compared to the ion density, the high value of Z gives strong coupling between the grains. Note that the floating potential and hence the value of Z will be reduced by the competition for electrons at high N referred to earlier. However it is believed that the required strong coupling conditions may have been achieved in the low pressure, low radio frequency argon discharge to reach the liquid dust form. Using the scattered light from the laser various structures can be observed. A liquid or colloid-type behavior of the larger dust particles is observed on a frequent basis after the discharge has been operated for tens of minutes.The dust appears and acts like a viscous fluid and displays collective behavior. Spectrum analysis of the scattered light shows that there is no random motion scattering such as is observed in the room air. The particle fluid responds to perturbations with a time constant of a few seconds and it appears to be nearly critically damped. Photographs show that when one has a high density layer of dust outside the electrode sheath, the dust layer develops its own sheath whose thickness is almost the same as that of the electrodes. For this to happen, the interparticle distance must be less than the Debye length. Recently, direct evidence of condensation has been obtained by H. Thomas (26) who seeded a discharge with particles large enough to permit in-situ microscopy and demonstrated their organization into a thin lattice given appropriate plasma conditions. There are many conditions of the nonideal and ideal plasmas with charged particulates or condensed dispersed phases (27) that are accessible. The high electron density nonideal plasma relates to the electron plasma of solid state and liquid metals, the superdense matter of the sun and collapsed stars, and to laser and charged particle beam interactions with materials. Normally the non-ideal plasma in gases in the laboratory is only formed under transient highly energetic conditions. The observed trapping of dust particles in a simple rf discharge is almost time-independent and thus gives rise to a wide range of analogous phenomena of multiphase plasmas that can be conveniently studied. Depending on the relative concentrations, particle sizes, and work functions of the material of the particles, the entire range of plasma states from a Debye plasma to a strongly non-ideal plasma can be realized.

## 7. Removal of particles

The particles can be easily removed from the plasma by switching the discharge off. Then, within millisecs the particles lose most of their charge and fall out of the plasma. If the substrate is mounted vertically or to the upper electrode, the particles usually do not interfere with the wafer process, providing the particle loading was not severe. The same results can be achieved by introducing a small amount of azimuthal asymmetry that permits the particles to leak-out of the electrostatic trap formed by the sheath fields and the ambipolar fields of the plasma. Selwyn et al.(1) have demonstrated that the asymmetry can be introduced by grooves in the electrode on which the substrate sits, and that these grooves can be made such that they convey the particles to the pumping port. A further way, which has been studied by several researchers (28,29) is to modulate the applied rf signal at low kilohertz frequency. This method has the advantage in that it is easily implemented, the system permits the negative ions to diffuse to the walls, and the dust never gets the opportunity to grow.

**Acknowledgements:** -The author acknowledges much inspiration from discussions on dust years ago with the late K. G. Emeleus. He also thanks his WPAFB colleagues B. N. Ganguly, P. D. Haaland, and J. Williams, and A. Bouchoule, D.B. Graves, A.A.Howling, M.J. Kushner, and G.S Selwyn for reprints and discussions,

**References**

1. G. S. Selwyn, J. E. Heidenreich, and K. L. Haller, Appl. Phys. Lett., **57**, 1876 (1990).
2. G. S. Selwyn, J. S. McKillop, K. L. Haller, and J. J. Wu, J. Vac. Sci. Tech., **A8**, 1726 (1990).
3. G. S. Selwyn,, J.,Singh, and R. S. Bennett, J. Vac. Sci. Tech., **A7**, 2758 (1989).
4. A. Bouchoule, A. Plain, L. Boufendi, J.Ph. Blondeau, and C. Laure, J. Appl. Phys.**70**, 1991 (1991).
5. J. L. Petrucci and C. Steinbruchel, Proc 8th Symp. Plasma Process., Electrochem. Soc., 219 (1990).
6. B. N. Ganguly, A. Garscadden, J. Williams, and P. D. Haaland, J. Vac. Sci. and Technology **A11**, 1119 (1993).
7. A. A. Abraham, 1974 "Homogeneous Nucleation Theory", Academic Press, New York
8. J. R.Heath, 1992 in "Fullerenes" eds G. S. Hammond and V. J. Kuck, ACS Symposium Series 481
9. L. F. Boufendi, A. Bouchoule, R. K. Porteous, J. P. Blondeau, A. Plain, and C. Laure J.Appl. Phys. **73**, 2160 (1993 ).
10. A. A.Howling, L. Sansonnens, J. L. Dorier and Ch. Hollenstein, J. Phys. D. **26**, 1003 (1993)
11. J. P. Boeuf, Phys. Rev., **A46**, 7910 (1992)
12. M. J. McCaughey and M. J. Kushner, Appl. Phys. Lett. **55**, 951 (1989)
13. R. M. Roth, K. G. Spears, G. D. Stein,and G. Wong, Appl. Phys. Lett.,**46**, 253 (1986).
14. S. G. Geha, R. N. Carlile, J. F. O'Hanlon, and G. S. Selwyn,J Appl. Phys. **72**, 374 (1992).
15. C. K. Goertz, Rev. Astrophys., **27**, 271 (1989).
16. E. C. Whipple, T. G. Northrop, and D. A. Mendis, J. Geophys. Res. **90**, 7405 (1985)
17. H. L. F. Houpis and E. C. Whipple, J. Geophys. Res., **92**, 12057 (1987)
18. E. J. Opik, Irish Astronomical Journal, **4**, 84 (1956).
19. E. C. Whipple, Rep. Prog. Phys., **44**, 1197 (1981).
20. D. A. Buffat and J. P. Borel, Phys. Rev. **A13**, 2289 (1976).
21. J. E. Daugherty, R. K. Porteous and D. B. Graves, J. Appl. Phys., **73**, 1617 (1993)
22. K. G. Emeleus, and A. C. Breslin Int. J. Electronics, **29**, 1 (1970).
23. R. J. Gould and E. E. Salpeter, Astrophys J. **138**, 393 (1963)
24. H. Ikezi, Phys. Fluids, **29**, 1764 (1986).
25. S. G. Brush, H. L. Sahlin and E. Teller, J. Chem. Phys., **45**, 2102 (1966)
26. H. Thomas, lecture at Wright-Patterson AFB, July 1993 and these proceedings.
27. V.E. Fortov, and I.T. Iakubov, "Physics of Nonideal Plasma", Hemisphere Publications, (1990).
28. J.T. Verdeyen, J. Beberman, and L. Overzet, J. Vac. Sci. Technol., **A8**, 1851 (1990).
29. Y. Watanabe, M. Shiratani and H. Makino, Appl. Phys. Lett., **53**, 1263 (1990).